Formation Control for Multi-Domain Autonomous Vehicles Based on Dual Quaternions

Ignacio Mas*†, Patricio Moreno*‡§, Juan Giribet*‡§ and Diego Valentino Barzi†
*Consejo Nacional de Investigaciones Científicas y Técnicas (CONICET), Argentina
†Instituto Tecnológico de Buenos Aires (ITBA), Argentina
‡Facultad de Ingeniería, Universidad de Buenos Aires, Argentina
§Instituto Argentino de Matemática "Alberto Calderón", CONICET, Argentina
Email: {imas, dvalenti}@itba.edu.ar; {jgiribet, pamoreno}@fi.uba.ar

***Abstract*—Unmanned networked multirobot systems have the potential to accomplish complex field tasks with minimum human intervention. Motion coordination of vehicles that operate in different domains (land, sea, air) is one of the problems that need to be addressed to achieve such a goal. This article presents a representation method based on dual quaternions for leader-follower formation control architectures. This representation offers the most compact and computationally efficient screw transformation formalism and can be used to describe rigid body motions because they simultaneously describe positions and orientations with only eight parameters. A controller in dual quaternion formation space is proposed and analyzed. Computer simulation results and experimental tests applied to the task of escorting an UGV with UAVs are shown to verify the functionality of the proposed system.**

I. Introduction

The concept of multiple robots working together in some coordinated fashion has been a topic of great interest in recent years. The ability to distribute tasks has the potential to increase performance, capabilities and tolerance to faults. This is particularly relevant when the robots operate in different domains as each vehicle inherently posses distinctive capabilities. We define domain as the environment the robot operates in (i.e. land, sea, or air) [1].

Examples of mission where these augmented features may result in a significant advantage include search and rescue operations, precision farming, forest fire control, asset surveillance and monitoring, convoy escorting and patrolling, etc.

Many formation control techniques have been developed over the years for mobile robot coordination. Some of them rely on biologically inspired behaviors [2], while others rely on leader-follower architectures [3], virtual structure definitions [4], virtual kinematic mechanisms [5], and potential field configurations [6].

Leader-follower configurations are the most common formation control technique found in the literature given its simplicity of specification: one designated leader follows a specified path and the rest of the vehicles' positions are specified relative to such leader or to other vehicles that ultimately depend on the leader. Additionally, this method allows for a distributed control scheme, as only local information may be needed to establish relative robot positions. Lastly, graph theory gives a convenient mathematical background to define formations and their communication paths in a formal manner.

When applied to formations of vehicles operating in three-dimensional space, although some authors limit the definition to formation parameters projected onto the plane –considering only range and bearing [7]– the typical leader-follower implementation relies on spherical coordinates to define range, azimuth and elevation of a follower with respect to a leader. In some works Cartesian distances between the leader and the followers are used [8].

Some authors have proposed formation control representations that rely on quaternions for representing the attitude of each individual robot with respect to a global frame [9] or with respect to a leader vehicle serving as an orientation reference [10].

In this article, we present a leader-follower formation definition based on dual quaternions. Dual quaternions offer the most compact and computationally efficient screw transformation formalism [11] and can be used as a representation to describe rigid body motions because they simultaneously describe positions and orientations with only eight parameters [12]. Similar to homogeneous transformation matrices, they can describe a complete rigid motion with a single mathematical object. Hence, a sequence of rigid motions is represented by a sequence of dual quaternion multiplications. The formation definition proposed in this article represents the position and orientation of the leader with a dual quaternion and the relative position and orientation of each follower with respect to the leader with additional dual quaternions.

To validate the proposed method, we choose the task of escorting an unmanned ground vehicle (UGV) with one or more unmanned aerial vehicles (UAVs). Therefore, the mission consisting on a UGV following a reference trajectory while UAVs fly around it in some specified manner is taken as a case study. This application is of particular interest to us due to its multi-domain nature.

Relative to previous work by the authors [13], this article extends the concept of representing position, shape, and size of the formation with dual quaternions to the leader-follower technique. Applying this concept to leader-follower formations, opens the door to a system definition that is scalable,

which can potentially be implemented with formations of large numbers of robots. Furthermore, this work validates the approach with experimental results while previous work only presented computer simulations.

This article is organized as follows. Section II describes the formation control methods commonly found in the literature. Section III presents the formation approach proposed and proves its stability in the sense of Lyapunov. Section IV shows results of the proposed method on computer simulations and on an experimental testbed, taking the task of aerial escorting of a ground vehicle as case study. Finally, Section V draws the conclusions.

II. Background

An important aspect of the formation control of mobile robots is the technique used to coordinate the motions of the individual vehicles. A wide variety of methods have been developed, drawing on work in diverse fields such as biology [14] or game theory [15] and applicable to robotic missions throughout land, sea, air, and space. The most common techniques include artificial potential fields that establish attraction and repulsion forces between robots [16], which have also been combined with behavioral primitives to react to the environment [17]. Another method relies on the definition of a virtual structure, where each robot tracks a particular node of the structure. The concept of a virtual kinematic mechanism that can be rotated, articulated and scaled over time has also been explored [5].

Swarm-like formation control methods [18], [19], focus on the benefits of abstracting to a low dimensional representation. Robots are usually only statistically bounded to certain region in space, and their precise location can not be specified. This is of great benefit for very large numbers of agents but its performance is limited when specific spacial requirements for each robot are needed. Additionally, the use of swarm techniques are typically limited to formations of homogeneous robots, and they are not applied to multi-domain systems.

The most commonly adopted method in the area of formation control is the leader-follower technique, in which follower robots control their position relative to a designated leader [20], [21], [22], [23]. A variant of this is leader-follower chains, in which follower robots control their position relative to one or more local leaders, which, in turn, are following other local leaders in a network that ultimately is led by a designated leader [24].

III. Dual quaternion formation definition

Dual quaternions have recently been used in different applications such as control of single free rigid bodies [25], cooperative manipulator arms [12], and group coordination of UAVs [26] and spacecrafts [27], [28].

A dual number is defined as $\hat{\alpha} = a + \epsilon b$ with $\epsilon^2 = 0$, but $\epsilon \neq 0$, where a and b are real numbers, called the principal part and the dual part, respectively. A dual quaternion can be treated as a dual number with quaternion components, i.e., $\hat{\mathbf{q}} = \mathbf{q}_p + \epsilon \mathbf{q}_d$, where $\mathbf{q}_p$ and $\mathbf{q}_d$ are quaternions.

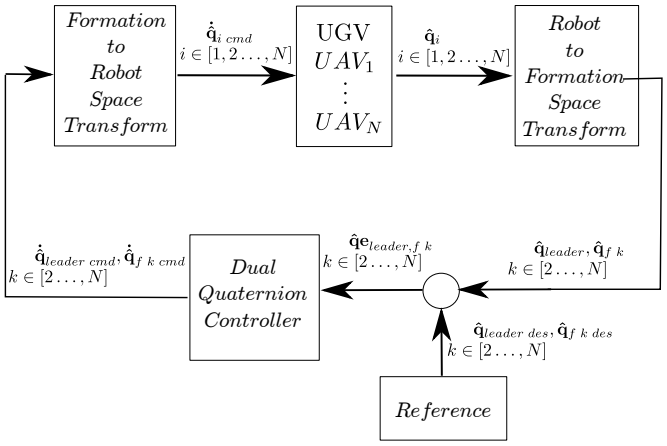

Fig. 1. Leader-Follower Dual Quaternion Controller Block Diagram

The dual quaternion $\hat{\mathbf{q}} = \mathbf{q} + \epsilon\frac{1}{2}\mathbf{p} \circ \mathbf{q}$ –where $\circ$ is the quaternion product– represents a rigid motion where the principal part $\mathcal{P}(\hat{\mathbf{q}}) = \mathbf{q}$ is a unit quaternion that represents the rotation and the dual part $\mathcal{D}(\hat{\mathbf{q}}) = \frac{1}{2}\mathbf{p} \circ \mathbf{q}$ is a quaternion that indirectly represents the translation. The translation can be retrieved using dual quaternion operation $\mathbf{p} = 2\mathcal{D}(\hat{\mathbf{q}}) \circ \mathcal{P}(\hat{\mathbf{q}})^*$, where $\mathbf{p} = (0, x, y, z)^T$ and $(.)^*$ represents the conjugation operation for quaternions. In the same way as it is done for dual numbers, it is possible to extend the operation defined for quaternions to dual quaternions. Moreover, as a quaternion can be expressed as a scalar component and a vector component, i.e. $\mathbf{q} = (q_0; \mathbf{q}_v)$, the dual quaternion $\hat{\mathbf{q}}$ can also be expressed as $\hat{\mathbf{q}} = (q_{p0}; \mathbf{q}_p; 0; \mathbf{q}_d)$. Notice that the scalar component of the dual part $\mathcal{D}(\hat{\mathbf{q}}) = \frac{1}{2}\mathbf{p} \circ \mathbf{q}$ is zero because the scalar component of $\mathbf{p}$ is zero.

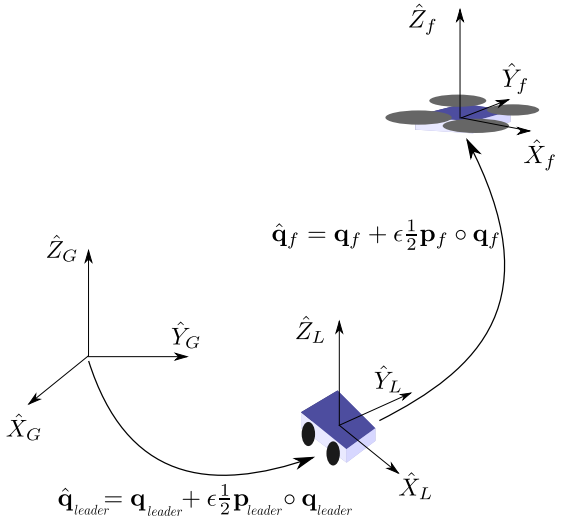

Fig. 2. Proposed leader-follower formation definition based on dual quaternions

We propose a specification of the formation in a space composed of the pose (position and attitude) of the leader and the relative pose of the followers with respect to the leader. Next, we propose a controller that operates on this

new space, minimizing the errors accordingly. Compensation signals generated by the controller are then transformed to the space of the vehicles to be applied to the system. Figure 1 shows the architecture of the controller.

Given a dual quaternion representation of the i^{th} robot's position and orientation: $\hat{\mathbf{q}}_i = \mathbf{q}_i + \epsilon\frac{1}{2}\mathbf{p}_i \circ \mathbf{q}_i$ where $\mathbf{q}_i$ is the quaternion representing the orientation and $\mathbf{p}_i = (0, x_i, y_i, z_i)$ represents its position, then, without loss of generality, designating robot 1 as a leader and robot $k \in [2\ldots, N]$ as a follower, we can define

$$\hat{\mathbf{q}}_{leader} = \hat{\mathbf{q}}_1 \quad (1)$$

$$\hat{\mathbf{q}}_{f\ k} = \hat{\mathbf{q}}_k \circ \hat{\mathbf{q}}_1^*, \quad (2)$$

where $\hat{\mathbf{q}}_1^*$ is the dual quaternion conjugate of $\hat{\mathbf{q}}_1$.

Equations 1 and 2 can be interpreted as a kinematic transformation ξ such that

$$\xi = \begin{bmatrix} f_l(\hat{\mathbf{q}}_1, \hat{\mathbf{q}}_k) \\ f_k(\hat{\mathbf{q}}_1, \hat{\mathbf{q}}_k) \end{bmatrix}_{k=2,\ldots,N} \quad (3)$$

that relates the representation in the space of the robots to the representation in the space of the formation. Figure 2 illustrates these relations. Additionally, an inverse kinematic relation can be defined as $\hat{\mathbf{q}}_1 = \hat{\mathbf{q}}_{leader}$ and $\hat{\mathbf{q}}_k = \hat{\mathbf{q}}_{f\ k} \circ \hat{\mathbf{q}}_{leader}$.

Given these definitions, a formation Jacobian matrix $J(\hat{\mathbf{q}}_1, \hat{\mathbf{q}}_k)$ that relates velocities in both spaces can be derived, obtaining $\dot{\xi} = J(\hat{\mathbf{q}}_1, \hat{\mathbf{q}}_k)[\dot{\hat{\mathbf{q}}}_1, \dot{\hat{\mathbf{q}}}_k]^T$. These expressions can be used in the dual quaternion formation space controller shown in Figure 1.

The proposed controller, based on previous works developed for cluster space architectures [13], considers the dual quaternion errors

$$\hat{\mathbf{q}}\mathbf{e}_m = \hat{\mathbf{q}}_m^* \circ \hat{\mathbf{q}}_{m\,des}; \quad m = \{leader, f\ k\}, \quad (4)$$

where $\hat{\mathbf{q}}_{m\,des}$ are the desired leader position and orientation and followers relative position and orientations. Equation (4) can be written with a decomposition in terms of the scalar and vector parts given by

$$\hat{\mathbf{q}}\mathbf{e}_m = (q_{p0_m}; \tilde{\mathbf{q}}_{p_m}; 0; \tilde{\mathbf{q}}_{d_m}); \quad m = \{leader, f\ k\}. \quad (5)$$

Theorem 1. *Let $K_{pw} \in \mathbf{R}^{3\times3}$ be a (strictly) positive definite matrix, the scalar gain $k_{dw} > 0$, and $\hat{\mathbf{q}}\mathbf{e}_m = (q_{p0_m}; \tilde{\mathbf{q}}_{p_m}; 0; \tilde{\mathbf{q}}_{d_m})$ the tracking error defined in equation* (4)*. If the following control laws are defined for the leader and the followers (where sgn is the sign function such that $sgn(0) = 1$):*

$$\dot{\hat{\boldsymbol{q}}}_{m\,cmd} = \frac{1}{2}\hat{\boldsymbol{q}}_{m\,cmd} \circ \begin{bmatrix} 0 \\ -sgn(q_{p0_m})K_{pw}\tilde{\mathbf{q}}_{p_m} \\ 0 \\ -sgn(q_{p0_m})k_{dw}\tilde{\mathbf{q}}_{d_m} \end{bmatrix}, \quad (6)$$

then, $\lim_{t\to\infty}|q_{p0_m}| = 1$ *(from where it follows that* $\lim_{t\to\infty}\tilde{\mathbf{q}}_{p_m} = 0$*), and* $\lim_{t\to\infty}\tilde{\mathbf{q}}_{d_m} = 0$.

Proof: Proposing the Lyapunov candidate function

$$V(\xi) = \sum_{m=\{leader,f\ k\}} \left(1 - q_{p0m}^2 + \tilde{\mathbf{q}}_{p_m}^T\tilde{\mathbf{q}}_{p_m} + \tilde{\mathbf{q}}_{d_m}^T\tilde{\mathbf{q}}_{d_m}\right), \quad (7)$$

its time derivative has the form

$$\dot{V}(\xi) = \textstyle\sum_{m=\{leader,f\ k\}} \cdots \left(-2q_{p0m}\dot{q}_{p0m} + 2\tilde{\mathbf{q}}_{p_m}^T\dot{\tilde{\mathbf{q}}}_{p_m} + 2\tilde{\mathbf{q}}_{d_m}^T\dot{\tilde{\mathbf{q}}}_{d_m}\right) \quad (8)$$

Notice that, the time derivative of the dual quaternion error $\dot{\hat{\mathbf{q}}}\mathbf{e}_m = (\dot{q}_{p0_m}; \dot{\tilde{\mathbf{q}}}_{p_m}; 0; \dot{\tilde{\mathbf{q}}}_{d_m}); m = \{leader, f\ \ k\}$ can be expressed as $\dot{\hat{\mathbf{q}}}\mathbf{e}_m =$

$$\frac{1}{2}\begin{bmatrix} -\tilde{\mathbf{q}}_{p_m}^T & 0 \\ q_{p0m}I_3 + \tilde{\mathbf{Q}}_{\times pm} & 0 \\ -\tilde{\mathbf{q}}_{d_m}^T & -\tilde{\mathbf{q}}_{p_m}^T \\ \tilde{\mathbf{Q}}_{\times dm} & q_{p0m}I_3 + \tilde{\mathbf{Q}}_{\times pm} \end{bmatrix}\begin{bmatrix} \omega_{pm\,cmd} \\ \omega_{dm\,cmd} \end{bmatrix} \quad (9)$$

where $\tilde{\mathbf{Q}}_{\times pm}$ and $\tilde{\mathbf{Q}}_{\times dm}$ are the cross-product operator skew-symmetric matrix form of $\tilde{\mathbf{q}}_{p_m}$ and $\tilde{\mathbf{q}}_{d_m}$ respectively, and I_3 is the (3×3) identity matrix. Additionally, $\omega_{pm\,cmd}$ and $\omega_{dm\,cmd}$ are defined by the controller as $\omega_{pm\,cmd} = -\text{sgn}(q_{p0_m})K_{pw}\tilde{\mathbf{q}}_{p_m}$ and $\omega_{dm\,cmd} = -\text{sgn}(q_{p0_m})k_{dw}\tilde{\mathbf{q}}_{d_m}$. These expressions can be substituted in (8) to obtain:

$$\begin{aligned}\dot{V}(\xi) = \sum_{m=\{leader,f\ k\}} \Big(&-\tilde{\mathbf{q}}_{p_m}^T|q_{p0m}|K_{pw}\tilde{\mathbf{q}}_{p_m}\cdots \\ &-\tilde{\mathbf{q}}_{p_m}^T|q_{p0m}|K_{pw}\tilde{\mathbf{q}}_{p_m}\cdots \\ &-\tilde{\mathbf{q}}_{p_m}^T\text{sgn}(q_{p0m})\tilde{\mathbf{Q}}_{\times pm}K_{pw}\tilde{\mathbf{q}}_{p_m}\cdots \\ &-\tilde{\mathbf{q}}_{d_m}^T\tilde{\mathbf{Q}}_{\times dm}\text{sgn}(q_{p0m})K_{pw}\tilde{\mathbf{q}}_{p_m}\cdots \\ &-k_{dw}|q_{p0m}|\tilde{\mathbf{q}}_{d_m}^T\tilde{\mathbf{q}}_{d_m}\cdots \\ &-\text{sgn}(q_{p0m})k_{dw}\tilde{\mathbf{q}}_{d_m}^T\tilde{\mathbf{Q}}_{\times pm}\tilde{\mathbf{q}}_{d_m}\Big). \end{aligned} \quad (10)$$

Since $\tilde{\mathbf{q}}_{p_m}^T\tilde{\mathbf{Q}}_{\times pm} = \tilde{\mathbf{q}}_{d_m}^T\tilde{\mathbf{Q}}_{\times dm} = 0$ and $\tilde{\mathbf{q}}_{d_m}^T\tilde{\mathbf{Q}}_{\times pm}\tilde{\mathbf{q}}_{d_m} = 0$, it follows that,

$$\begin{aligned}\dot{V}(\xi) = \sum_{m=\{leader,f\ k\}} \Big(&-2\tilde{\mathbf{q}}_{p_m}^T|q_{p0_m}|K_{dw}\tilde{\mathbf{q}}_{p_m} - \\ &|q_{p0_m}|k_{dw}\tilde{\mathbf{q}}_{d_m}^T\tilde{\mathbf{q}}_{d_m}\Big) \le 0 \end{aligned} \quad (11)$$

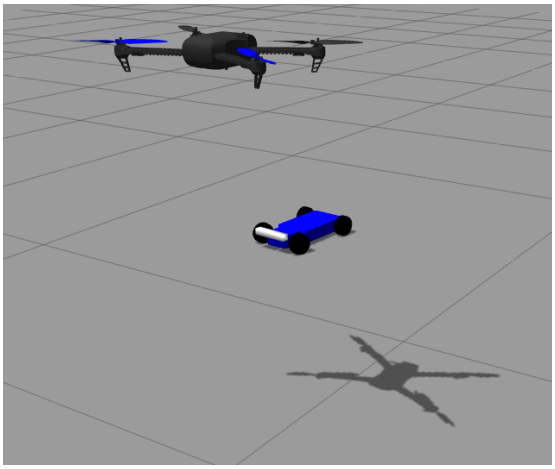

Fig. 3. ROS-Gazebo GUI models of UGV and UAV

Notice that, if $q_{p0_m} = 0$ (i.e., $\|\mathbf{q}_{p_m}\| = 1$) then $\dot{V}(\xi) = 0$. However from equation (9), if $q_{p0_m} = 0$, it follows that $0 = -\tilde{\mathbf{q}}_{p_m}^T \omega_{pm\,cmd} = \tilde{\mathbf{q}}_{p_m}^T K_{pw} \tilde{\mathbf{q}}_{p_m}$, which is not possible. Then $\dot{V}(\xi) = 0$ if and only if $\tilde{\mathbf{q}}_{p_m} = \tilde{\mathbf{q}}_{d_m} = 0$, rendering the system asymptotically stable. ■

IV. Results

The proposed system is implemented in computer simulations and on an experimental testbed.

The simulations are developed on the Robot Operating System (ROS) and Gazebo environment [29]. Within the simulation, the UAVs are modeled as IRIS multicopters from 3D-Robotics using a Gazebo plug-in developed by the Autonomous System Lab of ETH Zurich University. The UGV is modeled as an ackermann-drive vehicle using a Gazebo plug-in developed by the MIT Rapid Autonomous Complex-Environment Competing Ackermann-steering Robot (RACECAR) [30]. Each simulated UAV runs a Linux port of the PX4 autopilot firmware [31] with a MAVROS interface. Figure 3 shows the models of the vehicles in the Gazebo graphical user interface (GUI).

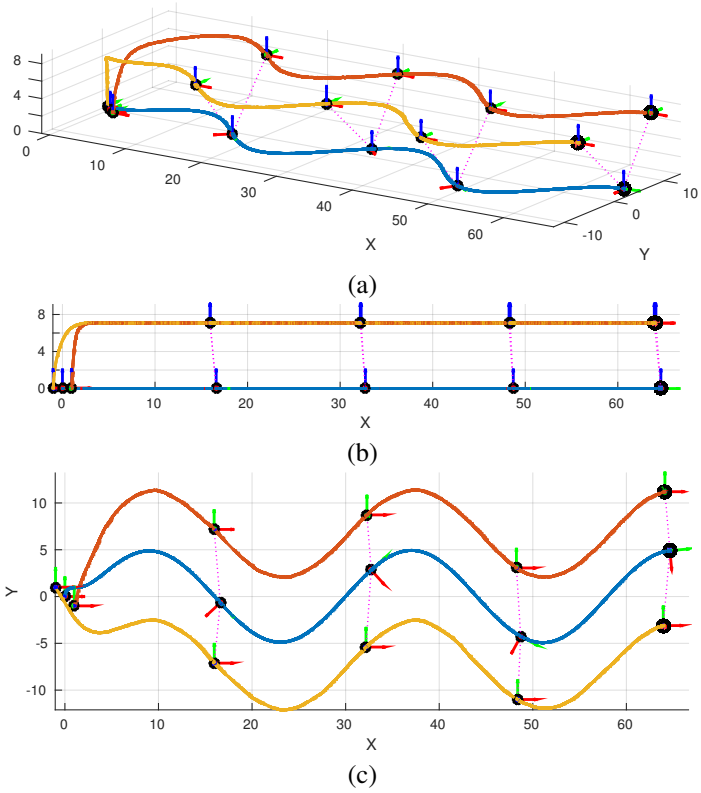

Fig. 4. Simulation result of a UGV following a sinusoidal trajectory and two UAVs escorting it. The UAVs maintain the relative position at an elevation of $45°$ and range of $10m$. (a) 3D view. (b) XZ plane side view. (c) XY plane top view.

The experimental testbed consists of a UGV based on a 1/16th scale RC buggy chassis with a Pixhawk autopilot, GPS receiver, and Bluetooth connection, and a UAV based on a 3D-printed quadrotor frame with a Pixhawk autopilot, GPS receiver, and a 433MHz Telemetry radio. Both vehicles are connected through MAVROS with a ground-based laptop computer running ROS. The computer implements the controller (6) with the architecture of Figure 1 in a MATLAB/Simulink environment and connects to ROS through the MATLAB Robotics Systems Toolbox.

A. Simulations Results

Two computer simulated scenarios are presented in this article. In the first scenario, the UGV (formation leader) follows a sinusoidal trajectory while two UAV followers escort it on each side at a distance (range) of 10m and an elevation angle of $45°$. The orientation (yaw) of the UAVs is constant (looking ahead) and the orientation of the UGV is a function of the commanded motion, given the nonholonomic constraint of the vehicle. Figure 4 shows the motion of the vehicles from different perspectives. Heading control on the UGV is implemented by commanding the vehicle steering according to $\phi = atan2(v_{x\,cmd}, v_{y\,cmd})$ at the output of the *Formation to Robot Space Transform* block in Figure 1. The dual quaternion controller gain is set to $K_{pw} = diag(0.3, 0.3, 0.3)$ and $k_{dw} = 0.3$.

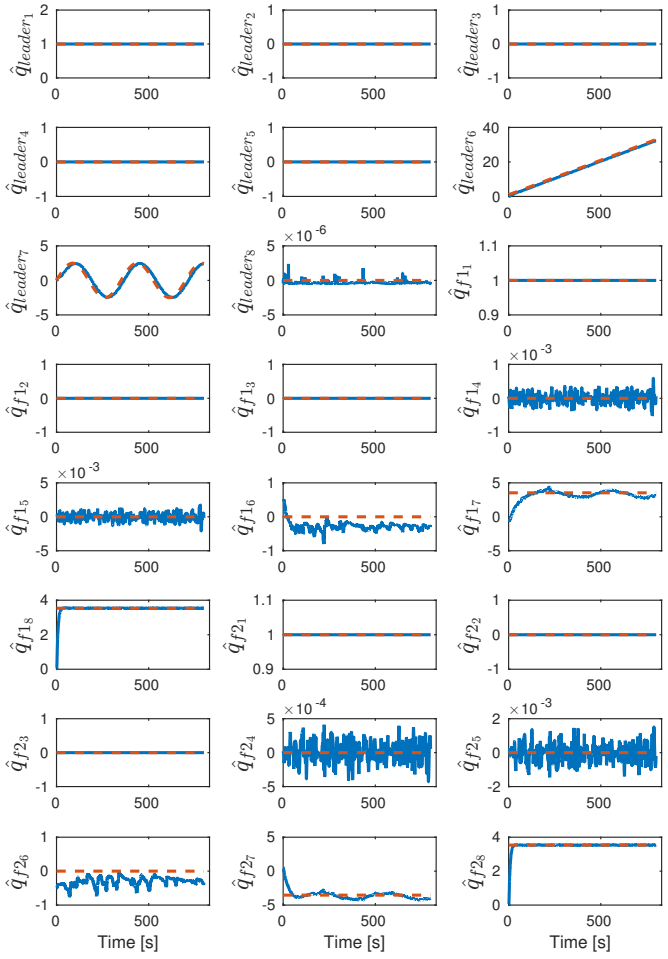

Fig. 5. Simulation results of a UGV following a sinusoidal trajectory and two UAVs escorting it (corresponding to Figure 4). Reference (dotted lines) and measured values (solid lines) over time of the dual quaternion coefficients.

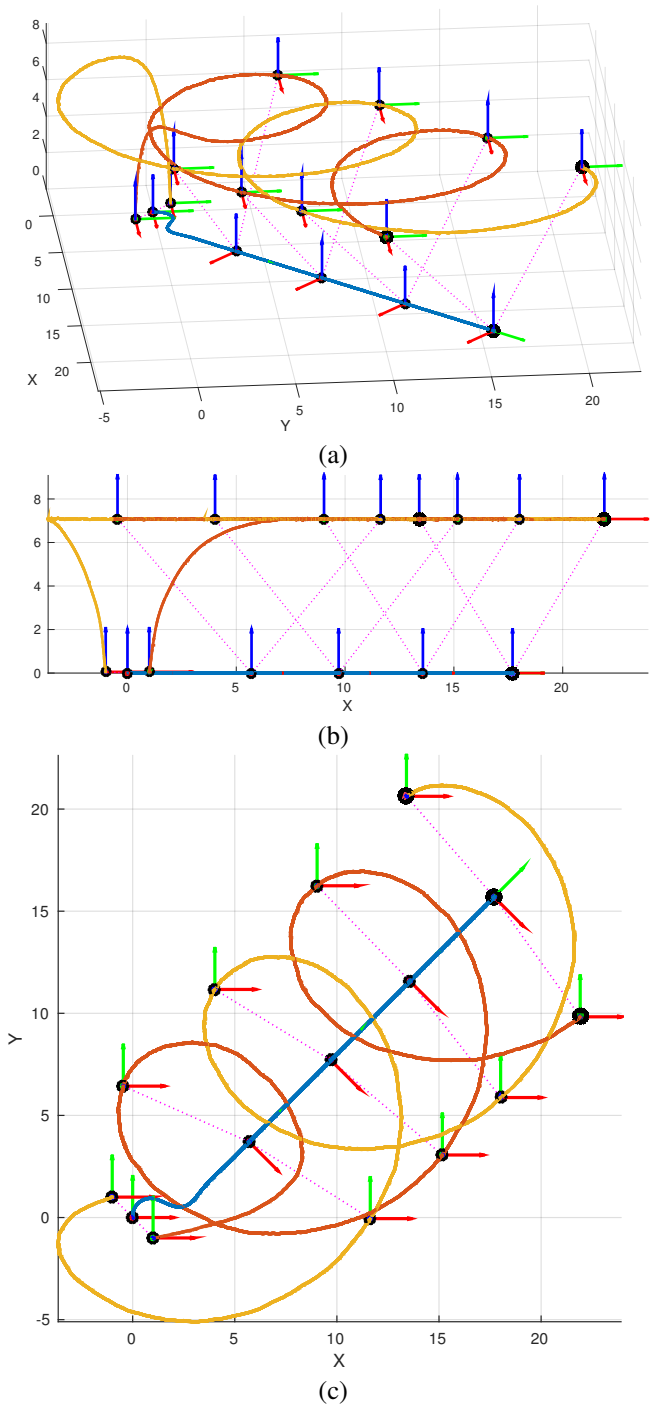

Fig. 6. Simulation result of a UGV following a rectilinear trajectory and two UAVs circling around it. The UAVs rotate around the posicion of the UGV at an elevation of 45° and range of $10m$. (a) Isometric view. (b) XZ plane side view. (c) XY plane top view.

Figure 5 shows the reference and measured values of the dual quaternion coefficients of the three vehicles. The first 8 coefficients $\hat{\mathbf{q}}_{leader_i}$ correspond to the UGV leader, where the first 4 coefficients –related to the orientation of the vehicle– are zero as the heading control is not controlled by the formation control framework but by the internal heading control described above, and the latter 4 coefficients –containing information of the vehicle's position– reflect tracking of the sinusoidal trajectory. The other two sets of coefficients $\hat{\mathbf{q}}_{f\,1_i}$ and $\hat{\mathbf{q}}_{f\,2_i}$ monitor the relative position of the UAV followers with respect to the leader.

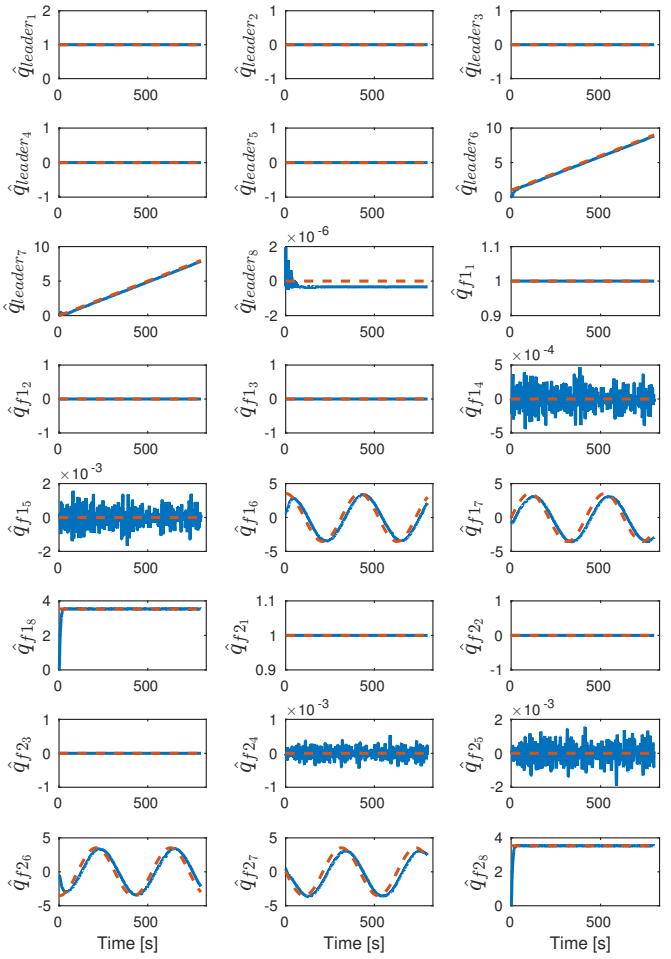

Fig. 7. Simulation results of a UGV following a rectilinear trajectory and two UAVs circling around it (corresponding to Figure 6). Reference (dotted lines) and measured values (solid lines) over time of the dual quaternion coefficients.

Fig. 8. Experimental testbed hardware: UGV and UAV

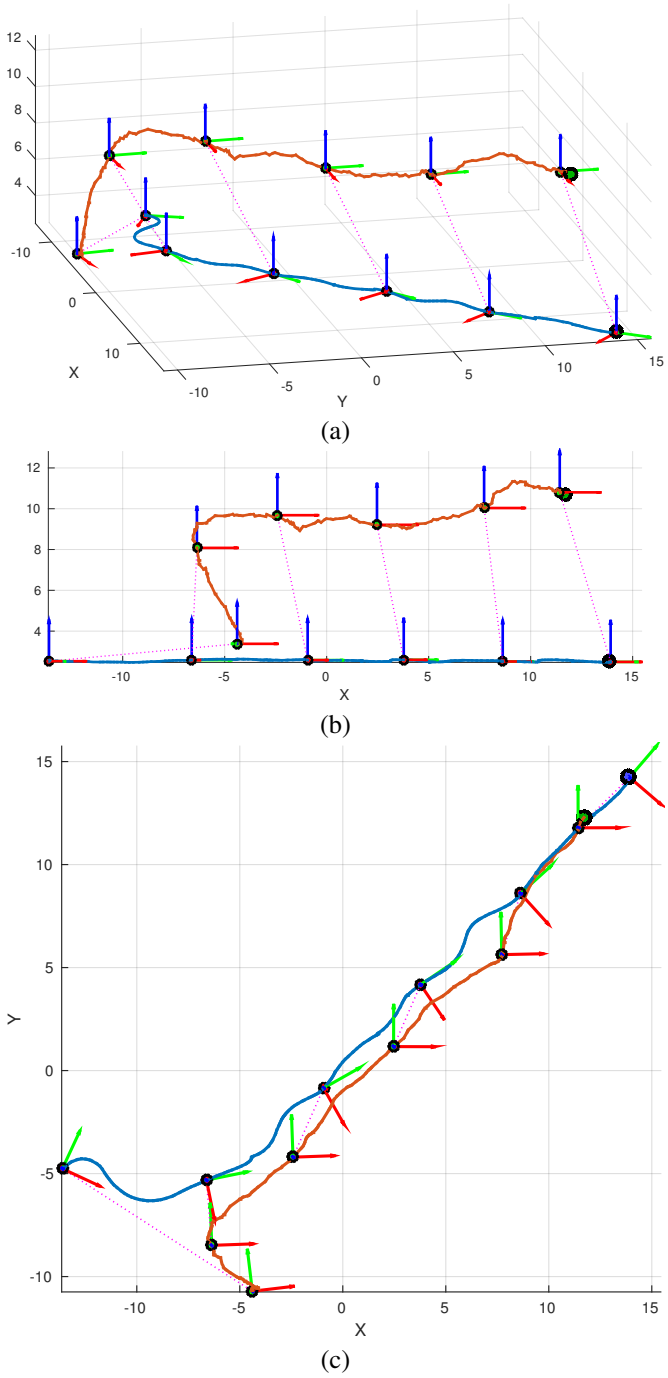

Fig. 9. Experimental result of a UGV following a rectilinear trajectory and a UAV flying above it at a constant relative altitude of $10m$. (a) Isometric view. (b) XZ plane side view. (c) XY plane top view.

The second simulation scenario consists of a rectilinear trajectory of the UGV while the two UAVs circle around it. The distance (range) between the UGV and UAVs is 10m and the elevation angle is $45°$. Figure 6 shows the vehicles' motion. The dual controller gains are similar to the previous scenario. Figure 7 shows the reference and measured values of the dual quaternion coefficients of the three vehicles.

In both simulations the vehicles track the reference trajectory successfully. Some steady state error can be seen due to the proportional nature of the controller.

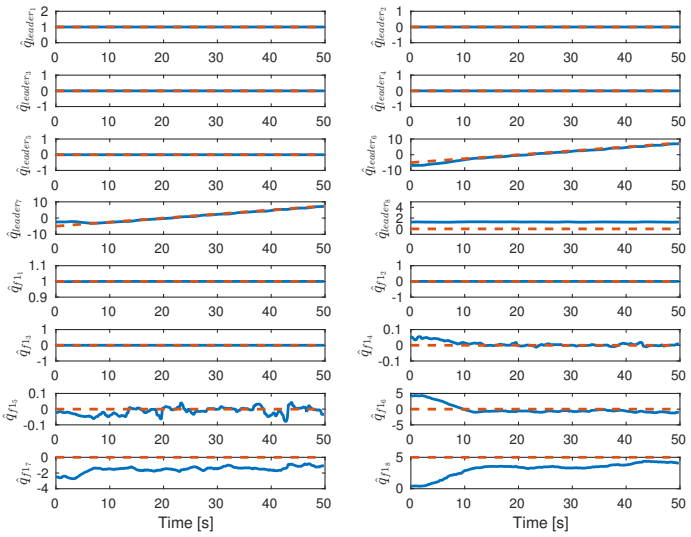

Fig. 10. Experimental results of a UGV following a rectilinear trajectory and a UAV flying above it at a constant relative altitude of $10m$ (corresponding to Figure 9). Reference (dotted lines) and measured values (solid lines) over time of the dual quaternion coefficients.

B. *Field Experiments*

Given the architecture of the system, the proposed controller can be seamlessly transitioned from the simulator to the hardware experimental testbed with minimal modifications. This is due to the fact that the interfaces with the real vehicles are similar to those of the simulator, as MAVROS and the PX4 firmware are common to both configurations. Furthermore, the gains of the controller are set equal to those used in the simulations. Two experimental results are shown in this article.

In the first experiment, one UGV follows a rectilinear trajectory and one UAV flies over it at a constant relative position, specifically 10 meters above the UGV while keeping a constant heading. Figure 9 shows the positions of the vehicles and Figure 10 indicates the reference and measured values of the dual quaternion coefficients.

In the second experiment, the UGV tracks an elliptical trajectory with a major axis of $30m$ and a minor axis of $12m$. The UAV keeps a constant relative position above it at an altitude of $10m$. Figure 11 shows the positions of the vehicles and Figure 12 indicates the reference and measured values of the dual quaternion coefficients.

In both cases the formation tracks the desired trajectories successfully. A lag between the position of the UGV and that of the UAV can be observed. As in the case of the simulation results, this is due to the steady state errors resulting from the proportional nature of the controller.

V. Conclusion

This article presented a leader-follower formation control architecture based on dual quaternion representations of the system and a dual quaternion controller that operates in the

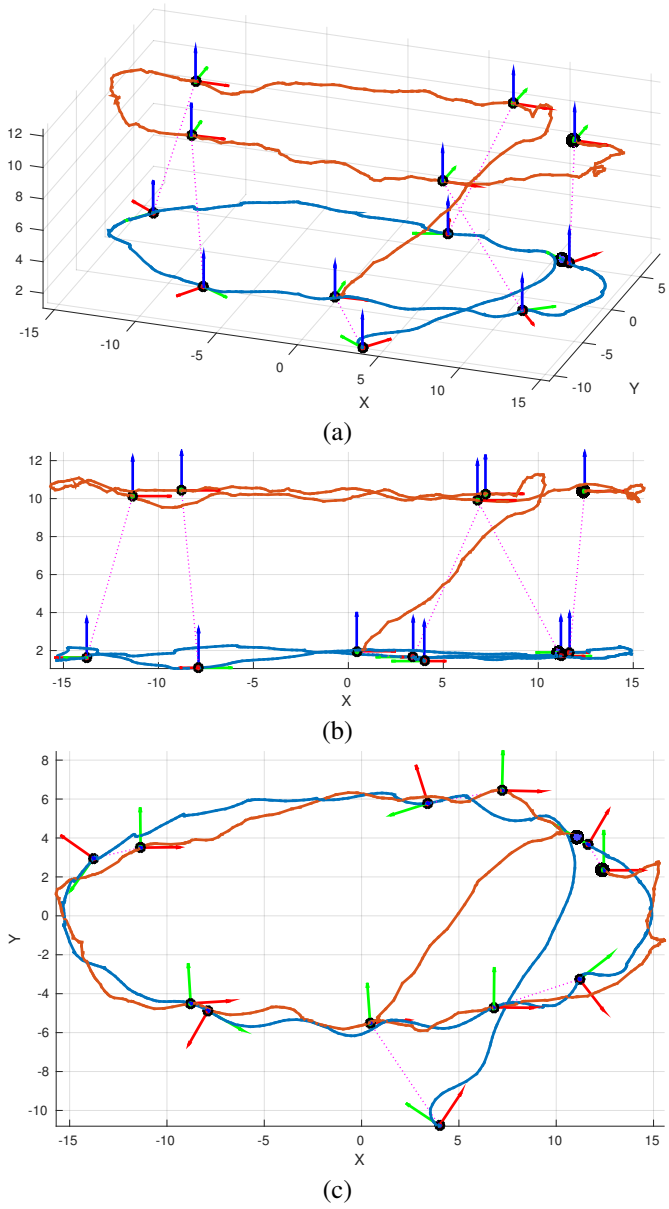

Fig. 11. Experimental result of a UGV following an elliptical trajectory and a UAV flying above it at a constant relative altitude of $10m$. (a) Isometric view. (b) XZ plane side view. (c) XY plane top view.

space of the formation. The stability of the controller was proven from a Lyapunov perspective.

Simulations and experimental results applied to the task of escorting a ground vehicle with unmanned aerial vehicles were presented to illustrate the validity of the approach. Furthermore, a seamless transition from the simulation environment to the experimental setup –which includes preserving controller gains syntonization– allows for system debugging and tunning before field deployment.

In terms of scalability, the proposed system lends itself to a distributed implementation. As this approach is based on the leader follower paradigm, the controller corresponding to each vehicle in the formation depends only on the state of that vehicle and that of the leader. Furthermore the Jacobian

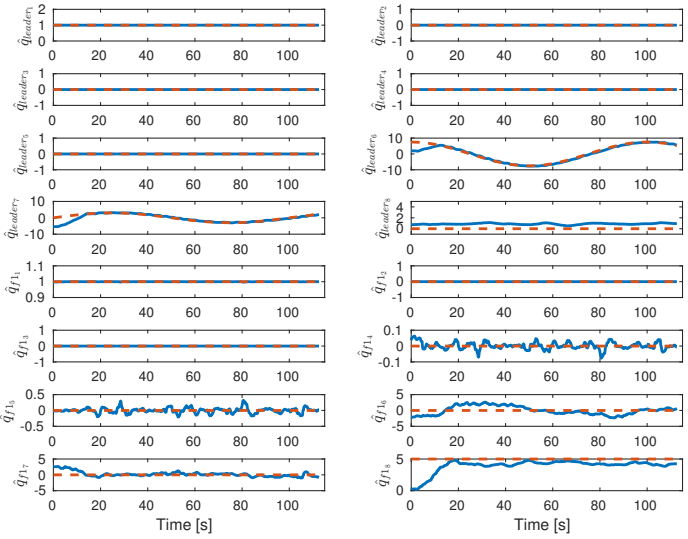

Fig. 12. Experimental results of a UGV following an elliptical trajectory and a UAV flying above it at a constant relative altitude of $10m$ (corresponding to Figure 11). Reference (dotted lines) and measured values (solid lines) over time of the dual quaternion coefficients.

matrix J has a block diagonal structure and the architecture of Figure 1 can be implemented in a distributed fashion [32].

Future work will focus on experimentation with a larger number of vehicles and the addition of features such as obstacle avoidance or aerial visual detection of objects of interest for active formation navigation.

ACKNOWLEDGMENT

The authors would like to thank Claudio Pose and Ezequiel Pecker Marcosig for their assistance operating the experimental testbed. This work has been sponsored through Agencia Nacional de Promoción Científica y Tecnológica, FONCYT PICT 2014-2055 (Argentina), Concurso de Iniciación a la Investigación ITBA 2016, Universidad Nacional de la Patagonia Austral (PI29/C066), and ITBA Grant ITBACyT-28.

REFERENCES

[1] F. Shkurti, A. Xu, M. Meghjani, J. C. G. Higuera, Y. Girdhar, P. Giguere, B. B. Dey, J. Li, A. Kalmbach, C. Prahacs, *et al.*, "Multi-domain monitoring of marine environments using a heterogeneous robot team," in *Intelligent Robots and Systems (IROS), 2012 IEEE/RSJ International Conference on*. IEEE, 2012, pp. 1747–1753.

[2] C.-H. Yu and R. Nagpal, "Biologically-inspired control for multi-agent self-adaptive tasks." in *AAAI*, 2010.

[3] Z. Lin, W. Ding, G. Yan, C. Yu, and A. Giua, "Leader–follower formation via complex laplacian," *Automatica*, 2013.

[4] K.-H. Tan and M. Lewis, "Virtual structures for high-precision cooperative mobile robotic control," *Intelligent Robots and Systems, IROS, Proceedings of the IEEE/RSJ International Conference on*, vol. 1, pp. 132–139, Nov 1996.

[5] C. A. Kitts and I. Mas, "Cluster space specification and control of mobile multirobot systems," *Mechatronics, IEEE/ASME Transactions on*, vol. 14, no. 2, pp. 207–218, April 2009.

[6] M. A. Hsieh, V. Kumar, and L. Chaimowicz, "Decentralized controllers for shape generation with robotic swarms," *Robotica*, vol. 26, no. 05, pp. 691–701, 2008.

[7] M. A. Kamel, K. A. Ghamry, and Y. Zhang, "Real-time fault-tolerant cooperative control of multiple uavs-ugvs in the presence of actuator faults," in *2016 International Conference on Unmanned Aircraft Systems (ICUAS)*, June 2016, pp. 1267–1272.

[8] W. Yu, G. Chen, and M. Cao, "Distributed leader–follower flocking control for multi-agent dynamical systems with time-varying velocities," *Systems & Control Letters*, vol. 59, no. 9, pp. 543–552, 2010.

[9] Q. Jia, G. Li, and J. Lu, "Formation control and attitude cooperative control of multiple rigid body systems," in *Intelligent Systems Design and Applications, 2006. ISDA'06. Sixth International Conference on*, vol. 2. IEEE, 2006, pp. 82–86.

[10] P. C. Wang, F. Hadaegh, and K. Lau, "Synchronized formation rotation and attitude control of multiple free-flying spacecraft," *Journal of Guidance, Control, and Dynamics*, vol. 22, no. 1, pp. 28–35, 1999.

[11] X. Wang, D. Han, C. Yu, and Z. Zheng, "The geometric structure of unit dual quaternion with application in kinematic control," *Journal of Mathematical Analysis and Applications*, vol. 389, no. 2, pp. 1352–1364, 2012.

[12] J. Dooley and J. McCarthy, "On the geometric analysis of optimum trajectories for cooperating robots using dual quaternion coordinates," in *Robotics and Automation, 1993. Proceedings., 1993 IEEE International Conference on*, 1993, pp. 1031–1036 vol.1.

[13] I. Mas and C. Kitts, "Quaternions and dual quaternions: Singularity-free multirobot formation control," *Journal of Intelligent & Robotic Systems*, pp. 1–18, 2016. [Online]. Available: http://dx.doi.org/10.1007/s10846-016-0445-x

[14] V. Kumar, N. E. Leonard, and A. S. Morse, *Cooperative Control: A Post-Workshop Volume, 2003 Block Island Workshop on Cooperative Control*. New York: Springer-Verlag, 2005.

[15] J. Barreiro-Gomez, I. Mas, C. Ocampo-Martinez, R. Sanchez-Pena, and N. Quijano, "Distributed formation control of multiple unmanned aerial vehicles over time-varying graphs using population games," in *2016 IEEE 55th Conference on Decision and Control (CDC)*, Dec 2016, pp. 5245–5250.

[16] P. Song and V. Kumar, "A potential field based approach to multi-robot manipulation," *Robotics and Automation. Proceedings. ICRA. IEEE International Conference on*, vol. 2, pp. 1217–1222, 2002.

[17] T. Balch and R. Arkin, "Behavior-based formation control for multirobot teams," *Robotics and Automation, IEEE Transactions on*, vol. 14, no. 6, pp. 926–939, Dec 1998.

[18] C. Belta and V. Kumar, "Abstraction and control for groups of robots," *Robotics, IEEE Transactions on*, vol. 20, no. 5, pp. 865 – 875, oct. 2004.

[19] R. Freeman, P. Yang, and K. Lynch, "Distributed estimation and control of swarm formation statistics," in *American Control Conference, 2006*, jun 2006, pp. 749–755.

[20] G. Mariottini, F. Morbidi, D. Prattichizzo, N. Vander Valk, N. Michael, G. Pappas, and K. Daniilidis, "Vision-based localization for leader-follower formation control," *Robotics, IEEE Transactions on*, vol. 25, no. 6, pp. 1431 –1438, dec. 2009.

[21] F. Yang, S. rong Liu, and F. Liu, "Cooperative transport strategy for formation control of multiple mobile robots," *Journal of Zhejiang University Science C*, vol. 11, no. 12, pp. 931–938, Nov 2010.

[22] R. Fierro, A. Das, J. Spletzer, J. Esposito, V. Kumar, J. Ostrowski, G. Pappas, C. Taylor, Y. Hur, R. Alur, I. Lee, G. Grudic, and B. Southall, "A framework and architecture for multi-robot coordination," *The International Journal of Robotics Research*, vol. 21, no. 10-11, pp. 977–995, Oct-Nov 2002.

[23] B. Smith, H. A., J. McNew, J. Wang, and M. Egerstedt, "Multi-robot deployment and coordination with embedded graph grammars," *Autonomous Robots*, vol. 26, no. 1, pp. 79–98, January 2009.

[24] A. Das, R. Fierro, V. Kumar, J. Ostrowski, J. Spletzer, and C. Taylor, "A vision-based formation control framework," *Robotics and Automation, IEEE Transactions on*, vol. 18, no. 5, pp. 813–825, Oct 2002.

[25] D.-P. Han, Q. Wei, and Z.-X. Li, "Kinematic control of free rigid bodies using dual quaternions," *International Journal of Automation and Computing*, vol. 5, no. 3, pp. 319–324, 2008.

[26] X. Wang, C. Yu, and Z. Lin, "A dual quaternion solution to attitude and position control for rigid-body coordination," *Robotics, IEEE Transactions on*, vol. 28, no. 5, pp. 1162–1170, 2012.

[27] H. Dong, Q. Hu, and G. Ma, "Dual-quaternion based fault-tolerant control for spacecraft formation flying with finite-time convergence," *ISA transactions*, 2016.

[28] J. Wu, K. Liu, Y. Gao, and B. Zhang, "6DOF quasi-optimal integral sliding mode control for satellite formation flying using dual quaternion," in *25th Chinese Control and Decision Conference (CCDC)*, May 2013, pp. 1764–1769.

[29] J. Meyer, A. Sendobry, S. Kohlbrecher, U. Klingauf, and O. Von Stryk, "Comprehensive simulation of quadrotor uavs using ros and gazebo," in *Simulation, Modeling, and Programming for Autonomous Robots*. Springer, 2012, pp. 400–411.

[30] MIT LIDS. Lab. (2016) MIT RACECAR project. [Online]. Available: http://fast.scripts.mit.edu/racecar/

[31] F. Furrer, M. Burri, M. Achtelik, and R. Siegwart, *Robot Operating System (ROS): The Complete Reference (Volume 1)*. Springer International Publishing, 2016, ch. RotorS—A Modular Gazebo MAV Simulator Framework, pp. 595–625.

[32] I. Mas and C. Kitts, "Centralized and decentralized multi-robot control methods using the cluster space control framework," *Advanced Intelligent Mechatronics (AIM), 2010 IEEE/ASME International Conference on*, pp. 115 –122, July 2010.